fire

MDPI

Article

Higher-Severity Fires Weaken Aboveground Biomass Recovery in Western US Conifer Forests

Nayani Ilangakoon [1,*], R. Chelsea Nagy [2,†], Virginia Iglesias [1,†] and Jennifer K. Balch [2,‡]

[1] Earth Lab, Cooperative Institute for Research in Environmental Sciences (CIRES), University of Colorado Boulder, 4001 Discovery Drive, Suite S348 611 UCB, Boulder, CO 80303, USA
[2] Environmental Data Science Innovation & Impact Lab (ESIIL), University of Colorado Boulder, 4001 Discovery Drive, Suite S348 611 UCB, Boulder, CO 80303, USA
* Correspondence: ginikanda.ilangakoon@colorado.edu
† These authors contributed equally to this work.
‡ Senior Author.

Abstract

Coniferous forests account for 78% of the western US forests and store a substantial amount of carbon. Wildfires significantly alter vegetation structure and associated forest carbon stocks. This study evaluates postfire biomass recovery trajectories (1984–2017) and total biomass accumulation in conifer forests that historically experienced low-severity, high-frequency fire regimes in the western US using recently launched Global Ecosystem Dynamic Investigations (GEDI) mission lidar data. All three ecoregions studied, including the Pacific Northwest (PNW), Southern Rockies (SR), and Northern Rockies (NR), show site-specific biomass recovery trajectories shaped by fire severity. The recovery trajectories were characterized by an initial decline and a variable gain with time since fire across the three ecoregions. Regions with low burn severity recovered to the unburned background state within the first three decades, while regions with higher burn severity only recovered in the Northern Rockies after five decades without fire. Moderate- and high-severity burned areas in both SR and PNW exhibited slow declines or sustained low biomass periods following fires, implying potential ecosystem transformation or an arrested state of lower biomass. Time since fire and fire severity were identified as the most significant drivers of postfire biomass recovery, likely because they reflect both reduced seed availability and the process of seedling establishment and regeneration. In addition, distance to unburned area, drought (measured using the Standardized Precipitation Evapotranspiration Index (SPEI)), elevation, and fire size were important drivers of biomass recovery. Our results demonstrate that all three ecoregions experienced a loss of overall biomass (15–23% (+/−40%)), with the largest losses occurring in the areas with high-severity burns (59% (+/−23%)) in the Southern Rockies compared to unburned forests within the first three decades. This study thus confirms GEDI's ability to assess disturbance-driven vegetation biomass dynamics and provides an open-science methodology that could be utilized for other regions. In conclusion, our study indicates that an increase in fire severity within low-severity, high-frequency fire regimes, beyond historically observed levels, results in greater carbon losses. It is therefore important to consider the effects of increases in fire severity on vegetation recovery trajectories to infer the future carbon potential in these ecosystems.

Keywords: fire regimes; fire severity; GEDI; recovery; biomass; chronosequence

Academic Editor: Jai Garg

Received: 5 January 2026
Revised: 12 February 2026
Accepted: 14 February 2026
Published: 24 February 2026

1. Introduction

Wildfires significantly influence global carbon cycling, ecosystem structure and functioning, and climate change [1,2]. Forest fires account for approximately 35% of global fire emissions and can shift these ecosystems, which store a substantial amount of carbon in vegetation and soil [3], from carbon sinks to carbon sources [4]. Decades of widespread fire suppression in the western United States have disrupted historical fire regimes, leading to excessive accumulation of live and dead fuels in some places [5]. These accumulated fuels, in combination with warming temperatures, increased human ignitions [6,7], and other disturbances [8,9], have driven recent increases in wildfire size and frequency across western US forests [10]. Increased wildfire activity causes substantial forest mortality, carbon emissions, and air quality degradation, and is associated with escalating fire suppression expenditures and property damage [11]. Thus, interest in the impacts of changing fire regimes across the western US and globally has increased, including short-term effects, such as poor air quality and home destruction, as well as long-term ecological impacts. Fire regimes are integral to maintaining the structure, composition, and ecological functions of forests, particularly in fire-adapted landscapes like western US conifer forests. A fire regime encompasses the typical frequency, severity, intensity, and spatial pattern of fires in a given ecosystem, which shape vegetation dynamics and nutrient cycles over time [12]. Historically, many conifer forests in this region, such as ponderosa pine (*Pinus ponderosa*) and mixed-conifer forests, evolved under low-severity, high-frequency fire regimes, which promote resilience by reducing surface fuel loads, enhancing nutrient recycling, and encouraging fire-adapted species regeneration [5]. However, a departure from these natural fire regimes due to fire suppression, land use changes, and climate warming has led to uncharacteristically large and high-severity fires in areas historically dominated by low-severity fires [8,13]. When fires exceed the natural severity for an area's historical regime, they can disrupt postfire recovery processes [14], impair carbon sequestration, and promote shifts to alternative ecosystem states, such as grassland or shrubland dominance [15,16]. Maintaining fire regimes that align with historical patterns is crucial to ensuring forest resilience and sustaining carbon storage, biodiversity, and ecosystem services in these landscapes. Thus, quantifying postfire carbon changes and recovery rates is essential to understand how quickly a fire-disturbed ecosystem can initiate carbon accumulation and recover to its initial state, the possibility of ecosystem state transitions [17,18], and how fires influence the global C budget [3,19].

Remotely sensed data have been extensively used to map different fire characteristics, including the burned area, burn severity, and postfire vegetation recovery [20]. Active remote sensing techniques such as lidar (Light Detection and Ranging) have been used to characterize postfire vegetation structure, aboveground biomass, and carbon stocks at various spatial scales [21–23]. The Global Ecosystem Dynamics Investigation (GEDI) spaceborne lidar system provides a novel approach to assessing postfire biomass recovery by delivering high-resolution, three-dimensional measurements of vegetation structure and biomass at a global scale. Unlike traditional remote sensing tools, which rely on optical and multispectral imagery to infer vegetation changes, GEDI directly measures aboveground biomass density (AGBD) with greater accuracy, particularly in capturing vertical forest structure and subtle changes in regrowth [24–26]. While spectral indices-based methods can highlight patterns of recovery and disturbance, they are limited in their ability to differentiate between regrowth in terms of structural biomass versus surface vegetation, where GEDI can explicitly quantify carbon stored in woody biomass, offering a more complete picture of recovery trajectories. Furthermore, GEDI enables large-scale monitoring of carbon dynamics, addressing gaps in literature studies that are often limited to localized field measurements or regional satellite analyses. This capability is particularly important

in understanding how forest ecosystems in the western US respond to increasingly frequent and severe wildfires [8,15]. This information is invaluable for informing forest management, carbon accounting, and climate mitigation strategies in fire-prone regions. In this study, aboveground biomass density metrics from the first-ever high-resolution spaceborne lidar sensor on the International Space Station; GEDI [24]; and three fire chronosequences representing three main ecodomains (Pacific Northwest (PNW), Northern Rockies (NR), and Southern Rockies and Colorado Plateau (SR)) in historically low-severity, high-frequency fire regimes were used to answer the following questions:

1. How quickly does forest biomass recover after fire, and how does the recovery rate vary across ecoregions?
2. To what extent do climatic conditions and fire characteristics (e.g., fire size and fire severity) explain postfire recovery in each ecoregion?
3. To what extent did wildfires in the western US change total aboveground biomass over a 34-year record?

Over the past few decades, all three ecoregions have been heavily influenced by fires of varying intensity and frequency [27]. The fire history, drought, vegetation, and topographic heterogeneity in the study domains provide a unique setting to evaluate postfire carbon recovery in mountainous, forested ecosystems within the historically low–moderate severity fire regime defined by the LANDFIRE Fire Regime Groups (FRG) product (LANDFIRE: Fire Regime Groups (2016) [28].

2. Methods

2.1. Study Area

The study area covers three National Ecological Observatory Network (NEON) ecodomains in the western US: PNW, NR, and SR (Figure 1a) [29,30]. Vegetation cover and composition in the three ecodomains are shaped by climate, elevation, and soil properties. Approximately 56% of the SR area is mixed forests characterized by ponderosa pine (*Pinus ponderosa*), lodgepole pine (*Pinus contorta*), aspen (*Populus tremuloides*), and pinyon–juniper (*Pinus edulis*, *Juniperus scopulorum*, *J. monosperma*, and *J. osteosperma*) [31].

The PNW ecodomains, which has a complex land use and disturbance history, is dominated by Douglas fir (*Pseudotsuga menziesii*) and other true fir species (e.g., *Abies grandis*, *Abies procera*, *Abies amabilis*, *Abies lasiocarpa*, *Abies concolor*, and *Abies magnifica*). Among many species, ponderosa pine (*Pinus ponderosa*), Douglas fir (*Pseudotsuga menziesii*), western larch (*Larix occidentalis*), western white pine (*Pinus monticola*), western redcedar (*Thuja plicata*), western hemlock (*Tsuga heterophylla*), grand fir (*Abies grandis*), and lodgepole pine (*Pinus contorta*) are present across the NR ecodomains [32].

2.2. Fire Events

Data on 393 fires within historically low–moderate-severity fire regimes within conifer forests dominated regions were obtained from the Monitoring Trends in Burn Severity (MTBS) fire occurrence dataset, fire boundary dataset, and burn severity mosaic datasets [20,28,33] between 1984 and 2017 (Figure 2). The regions of historically low–moderate severity fire regimes were selected using the LANDFIRE fire regimes product, where the percent replacement fire was less than 66.7%, and the fire return interval was 6–35 years. High-severity fire regimes were excluded due to an insufficient number of fire events to support chronosequence analysis. The National Land Cover Datasets (NLCD) between 1985 and 2016 were used to extract fires that occurred only within the Evergreen Forests (NLCD ID = 42) [34–36]. The NLCD class 42 represents pixels of evergreen forests that are dominated by trees greater than 5 m tall, and 75% of the tree species maintain their leaves all year. The selection of NLCD class 42 further allows us to use GEDI biomass

density metrics, which are less uncertain due to GEDI's capability to detect vegetation heights greater than 5 m at high accuracy [37].

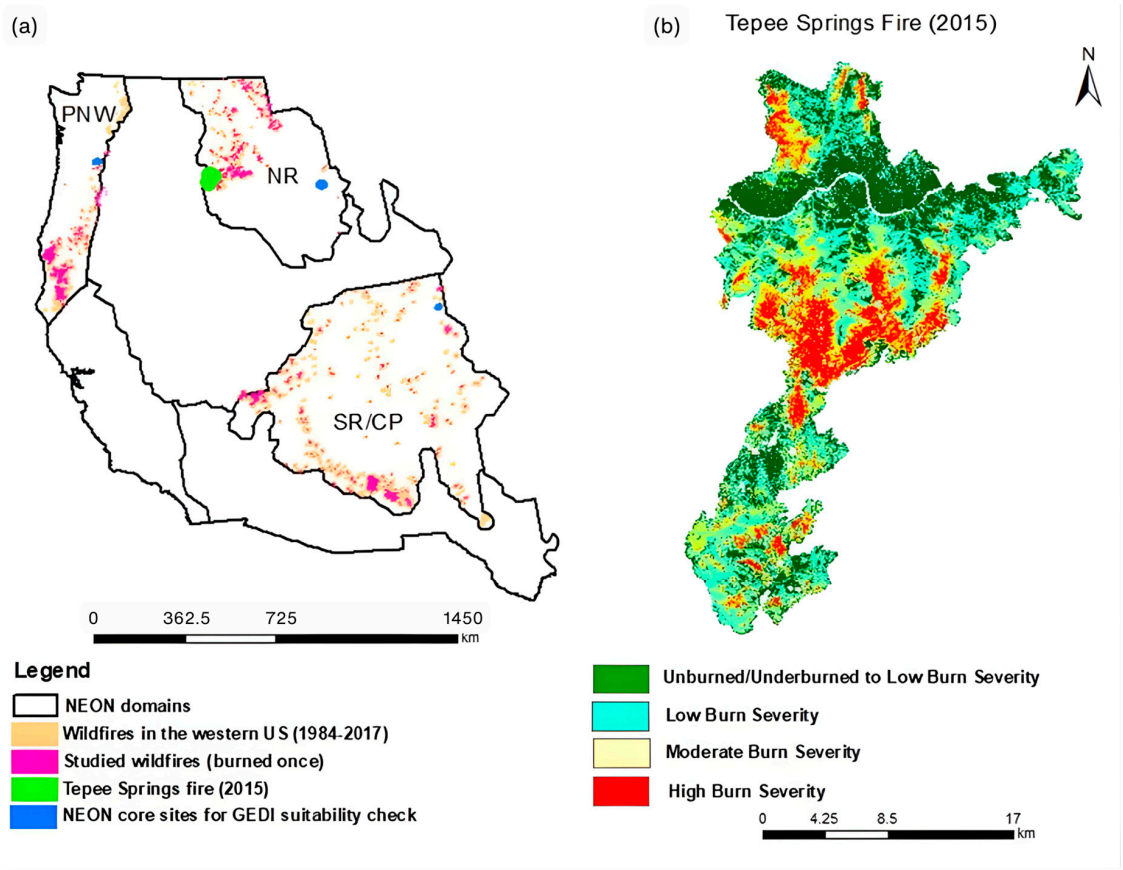

Figure 1. (**a**) Wildfires in the three western US ecodomains as reported in Monitoring Trends in Burn Severity (MTBS; 1984–2017). (**b**) MTBS burn severity within the Tepee Springs fire (2015).

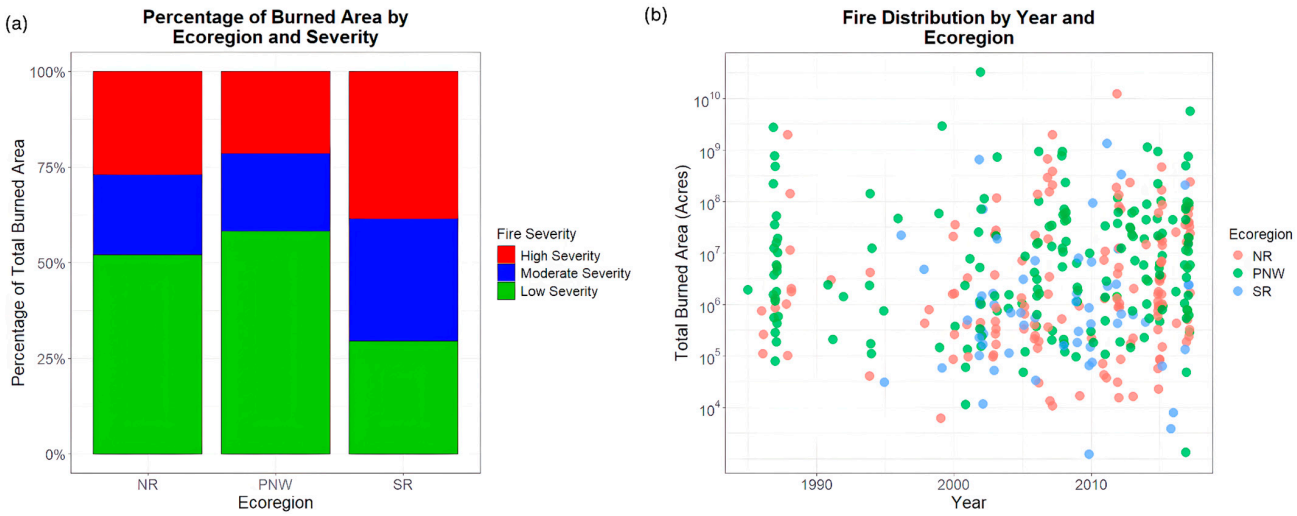

Figure 2. (**a**) Proportion of burned area by fire severity class (low, moderate, and high) for all fires occurring within low–moderate fire regimes ecosystems from each ecodomains. (**b**) Fire size and ignition year distribution of all fires in the low–moderate fire regimes used in this study. There were more fires in each ecodomains in the later decades (2000–2017).

The last land cover map prior to the fire of interest was used to select the prefire vegetation. From the selected fires, our study was constrained to areas that burned only

once and were within the low–moderate fire regime. For each fire event, the fire perimeter, fire size, and year of the fire were extracted. Using these data, the offset-corrected Relative Differenced Normalized Burn Ratio (RdNBR) was derived at the pixel level within burned areas using Google Earth Engine (GEE). Burn severity classes were assigned based on established RdNBR thresholds [38]. The overlap among severity classes across fires was assessed to verify that the reclassified severity metrics were comparable among fire events, enabling cross-fire analyses of burn severity effects [39]. Corrections and detailed analysis of MTBS data are described in the Supplementary Information (Supplementary Figure S1).

2.3. GEDI Data and the Postfire Recovery Metrics

This study was focused on the GEDI-derived aboveground biomass density (AGBD) metric, which shows measurable changes in biomass along the postfire period, and is widely used to estimate carbon. Specifically, GEDI 4A rasters in GEE were used for this study. GEDI Level 4A footprints were filtered using established quality criteria, including the L4 quality flag, degradation flag, waveform sensitivity, and plant functional type classification. Only footprints meeting all quality thresholds (l4_quality_flag = 1; degrade_flag = 0; AGBD > 0; sensitivity $\geq$ 0.90) and classified as evergreen needleleaf forest (PFT code = 1) were used for our analyses [25,40]. GEDI biomass density data for footprints within fires where the majority of the land cover was conifer forest (a total of 534,114 biomass pixels across the three ecodomains) were extracted. Each footprint was assigned a severity index based on the new severity classes calculated in the above section. Unburned points were selected from unburned locations within the last 50 years, according to the Combined wildland fire dataset [41] locations surrounding each fire within 2 km of the fire boundary (a total of 129,002 points). These unburned point locations were within the same fire regime group and belonged to NLCD class 42. AGBD data were collected for these unburned points and connected to the closest burned points to extract the biomass gain/loss with the fire event. Postfire recovery trajectories were developed based on biomass differences to the nearest unburned area. In addition to AGBD data, GEDI canopy height metrics were also downloaded. The canopy height metrics were also compared with high-resolution airborne lidar-based metrics from NEON sites representing each ecodomain for validation. The GEDI-derived canopy height and canopy-height–derived biomass estimates showed a strong agreement with NEON-based metrics, confirming the suitability of GEDI in this study (Supplementary Figure S2).

2.4. Climate Variables

The following variables were used in the analyses: the mean annual precipitation (mm), standardized precipitation evapotranspiration index (SPEI06—SPEI calculated using 6 months differences between precipitation and potential evapotranspiration), relative humidity, and vapor pressure deficit (VPD; kPa). Climate data layers representing each variable mentioned above between 1984 and 2017 were extracted from the Climatic Research Unit database [42,43], which provides data at 4 km resolution. To facilitate across-fire climate comparisons and account for their impact on postfire recovery, the selected climate variables were converted to postfire climate anomalies. Climate data were log-transformed to correct the data skewness. Then, the z-score or the climate anomaly was calculated for each climate variable (precipitation, SPEI-6, and VPD), following the equation below [44]:

$$Z = (\mu\_(post) - \mu\_(norm))/\sigma \quad (1)$$

where Z, μ_(post), μ_(norm), and σ are the Z statistic, postfire mean climate, mean climate normal between 1984 and 2017, and standard deviation of the climate normal between 1984 and 2017, respectively. To calculate the mean postfire climate for each fire, we extracted

values from each climate variable from one year after the ignition year until 2017. If more than one climate pixel was found within a single fire, the average was used, so that only one value per climate variable per fire was produced. Additional testing was performed to confirm whether climate variability differed more among years than among fires within the same year and ecodomain in order to evaluate the suitability of climate metrics for a space-for-time (chronosequence) substitution framework. Results from mixed-effects ANOVA models showed that interannual and regional variability in climate conditions substantially exceeded fire-to-fire variability within the same year. Supporting analyses using SPEI data are presented in Supplementary Figures S3 and S4.

2.5. Building Postfire Recovery Trajectories

Postfire recovery trajectories were built for three chronosequences, PNW, NR, and SR/CP (SR hereafter). Our study focused on fires where time since fire was between 1 and 33 years (1984–2017) to evaluate the recovery rates and trajectory. GEDI footprints were used as the sample unit in this study. The explanatory variable was the GEDI footprint-based biomass density. Biomass change with respect to the nearest unburned values was used as the recovery metric and was evaluated as a function of fire (severity, time since fire), site (elevation, distance to unburned area), and climate (precipitation, temperature, drought as represented by the SPEI, and relative humidity).

To identify the shape of the recovery trajectory (Q1), nonlinear models of Gompertz, Chapman–Richards, Michaelis–Menten, and polynomial functions were fitted to the original GEDI metric points using the R package "growthmodels" [45]. Our selection of non-linear models was based on visual inspection of the data distributions supported by evidence of nonlinear chronosequences of carbon recovery across a range of ecosystems [46,47]. Model performance was evaluated with Akaike Information Criterion (AIC) [48] and standard residual errors. In each ecodomain, the model that minimized both estimates was used to estimate recovery rates and the time required to recover to the background state.

To explore the role of fire size, climate, and fire severity on postfire vegetation recovery, Generalized Additive Models (GAMs) were used. GAMs can reveal both linear and nonlinear effects of climate anomalies on biomass change, with climate sensitivities and temporal trajectories differing among ecodomains of interest. GAMs also enable the use of region-specific smooth terms to characterize the climate tolerances and thresholds for ecodomains consistent with differential resilience to climate stresses. Given the non-normality of our data and the potential for linear and nonlinear effects of the predictors on recovery trajectories, data-driven models that allow the specification of the distribution of the response variable and the link function, such as GAMs [49], provide optimal tools for association estimation in our study. To assess the relative influence of the explanatory variables on GEDI-derived AGBD (recovery trajectories), a forward stepwise selection process was followed. That is, starting from a null model, we added predictors one at a time and compared the performance of the respective models based on their AIC. Structural metrics from undisturbed sites were used as the reference state to estimate the change in vegetation structure at each time step. The data were processed in R (R studio) using packages "nlme" and "drc" and "gam".

2.6. Postfire Biomass Gain/Loss

The biomass gained across severity gradients was estimated and compared with the biomass that the system may have had if the area had not burned. To estimate the biomass if the area had not burned, the average unburned biomass from each fire was multiplied by its area burned. As there were many unburned pixels both inside and surrounding each burned area, we consider this average biomass of the unburned pixels to be a conservative

estimate to represent the unburned biomass for each fire. The biomass gain within the burned area is the sum of the biomass calculated by the mean biomass of each fire severity category multiplied by the area burned at that severity for each fire. The percentage of biomass gain/loss as a function of fire in each ecodomains at each severity gradient was then calculated.

3. Results

3.1. Biomass Recovery Across Ecodomains

The mean biomass density of the unburned regions is 121 (+/−81) Mg/ha, 227 (+/−125) Mg/ha, and 76 (+/−46) Mg/ha for NR, PNW, and SR, respectively. The recovery trajectories are unique for each ecodomain and the severity category. In this study, biomass recovery is defined as the biomass difference (Mg/ha) from an unburned control or prefire baseline; positive values indicate biomass gain; negative values indicate biomass loss. In the Southern Rockies, low-severity fires in historically low- to moderate-severity fire regimes are associated with early postfire biomass stability and gradual recovery, consistent with resilient forest carbon dynamics (Figure 3a). Positive recovery (biomass increases) is observed after 15–20 years. Moderate-severity fires show a temporary decline in biomass immediately postfire but remain steady since then at a lower biomass state than the pre-burn. The higher-severity Southern Rockies fires in historically low- to moderate-severity fire regimes show a significant initial loss of biomass postfire, with a sharp dip reaching −20 Mg/ha. Since then, a continuous slow decrease has been observed within the first 10–15 years before it reaches a lower steady state compared to lower-severity fires, reflecting the greater damage caused by high-severity fires.

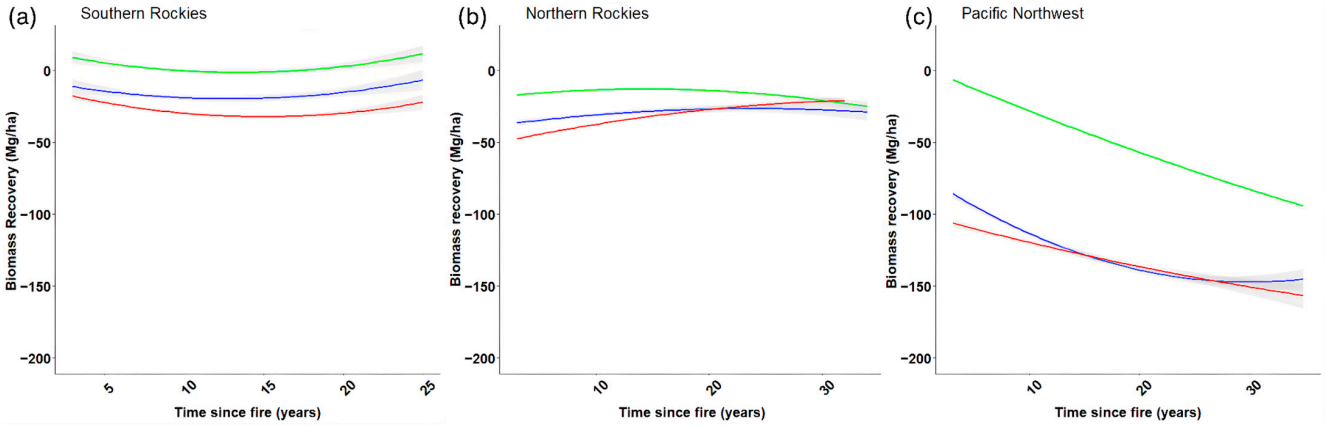

Figure 3. Biomass recovery trajectory postfire with respect to the pre-burned biomass across severity gradients. The solid-colored lines represent the mean recovery trajectory of each severity (green: low, blue: moderate, red: high), and the gray area at either side of the solid lines represents the 95% confidence interval. (**a**) Biomass recovery of the Southern Rockies, (**b**) Biomass recovery of the Northern Rockies, (**c**) Biomass recovery of the Pacific Northwest.

In the Northern Rockies (Figure 3b), the biomass recovery trajectories reflect different patterns than those from SR. After low-severity fires in the NR, biomass recovers steadily, but shows a slight decrease in later years. The biomass in the moderate-severity fires initially dips but then slowly increases during the first 30 years and levels off at a lower state than that of the unburned biomass. In contrast, the biomass of the higher severity burned areas initially reaches as low as −50 Mg/ha relative to the baseline biomass in the SR. Then, biomass recovers continuously at a slower rate, maintaining a positive trend for 20–30 years postfire. Interestingly, the higher-severity trajectory crosses the moderate-severity recovery trajectory around 20 years postfire.

In the Pacific Northwest (Figure 3c), in contrast to the other two regions, all three severity classes show a fairly continuous decrease in biomass postfire. In the low-severity fires, biomass recovery is relatively slow and stabilizes at a lower recovery rate compared to the Rockies.

While a positive recovery trend is possible, the Pacific Northwest shows less resilience to low-severity fires compared to the other two regions. The biomass of the moderate-severity fires in the PNW consistently declines over time for at least the first three decades before starting to pick up. The biomass loss in the higher-severity fires in the historically low- to moderate-severity fire regimes is substantial, reaching up to ~−150 Mg/ha compared to the unburned levels. Unlike the Rockies, no recovery is observed over time within the studied time frame from the baseline unburned areas, with biomass levels continuing to decline, highlighting significant ecosystem disruption and impaired recovery processes. This further suggests that both moderate- and high-severity fires have long-lasting impacts in the Pacific Northwest, especially on high-biomass regions after a fire.

3.2. Effect of Climate and Site Characteristics on Fire Recovery Trajectory

Figure 4 shows the partial effects of the most significant variables explaining (X axis) the biomass gain/loss in each ecodomain. The solid lines represent the effect of the predictor, and the dashed lines represent the 95% confidence interval. When considering all three ecodomains together, time since fire alone explained 50–60% of the biomass recovery. While the time since fire shows a nonlinear effect on postfire recovery, fire severity, elevation, distance to undisturbed areas, and fire size show a linear effect on the postfire canopy height gain (Figure 4). When considering each ecodomain as a separate unit, the important controlling factors were significantly different. In the Southern Rockies, a nonlinear relationship is observed with time since fire, where biomass recovery initially declines for the first ~10 years postfire but increases after ~15 years. This reflects the lagged recovery pattern commonly observed in fire-adapted ecosystems. Interestingly, the fire size shows a slight positive relationship, suggesting that larger fires may have slightly higher biomass recovery, likely due to enhanced regeneration of alternative vegetation in larger disturbed areas such as aspen [50]. The negative linear trend with fire severity shows a greater reduction in biomass, highlighting the detrimental effects of severe fires on forest recovery. The negative relationship with distance indicates that greater distances from unburned patches are associated with reduced biomass recovery.

In the PNW region, other than time since fire, elevation, fire severity, and fire size significantly controlled the postfire biomass gain. Based on our results, postfire recovery in PNW decreased drastically when the severity increased, reflecting the severe impacts of intense fires in this ecodomain. However, there is a slight positive relationship between biomass and the increase in elevation.

Similarly, the recovery trajectory of the NR region is also controlled by time since fire, fire severity, and elevation. This is the only region where drought (detected as SPEI) plays an important role in the recovery trajectory. Biomass declines immediately postfire but starts recovering steadily after ~10 years. A strong positive relationship is observed with the elevation, indicating better recovery at higher elevations. This may reflect cooler, wetter conditions at higher altitudes that favor regrowth. The negative trend in biomass with SPEI implies that drier conditions may hinder biomass recovery. The negative linear relationship with fire severity shows a significant biomass reduction when the severity increases.

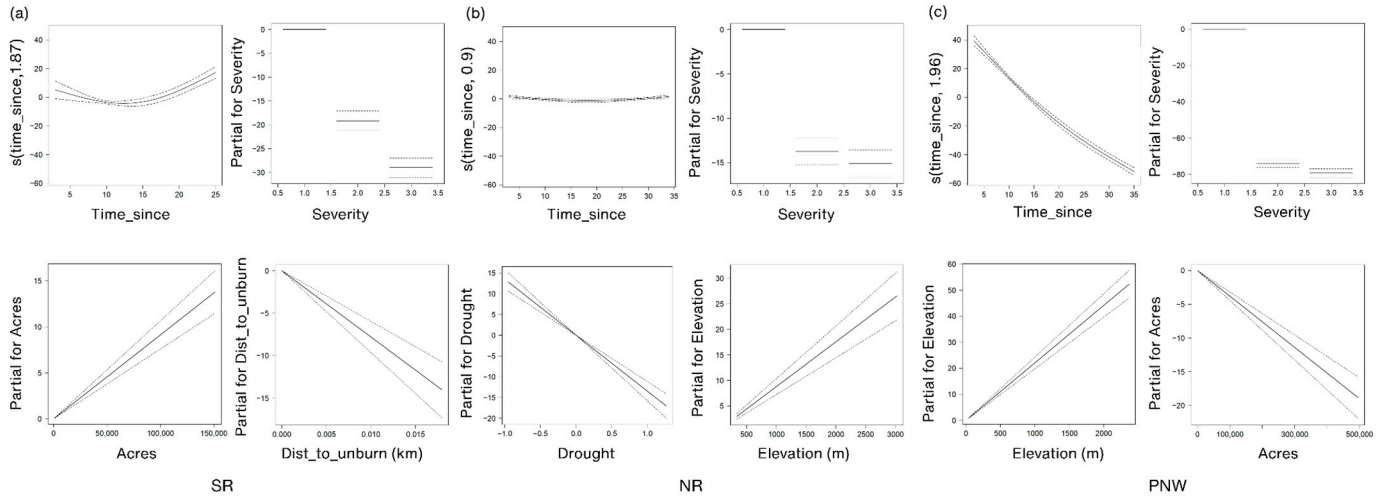

Figure 4. Partial effects of most significant variables explaining the postfire biomass recovery trajectory in (**a**) the Southern Rockies, (**b**) Northern Rockies, and (**c**) Pacific Northwest. The solid black lines show the mean effects in each ecodomain, while the areas within dashed lines around the solid lines represent the 95% confidence intervals for each partial effect. Severity was used as a categorical variable, as there were three distinct classes in our study. A negative trend in the partial effect indicates that increasing values of the predictor are associated with reduced postfire biomass recovery (e.g., increasing drought severity is associated with lower recovery potential in the Northern Rockies).

3.3. Postfire Biomass Stock in the Western US

Estimated total biomass shows a significant reduction compared to the unburned background state in all three ecodomains (Figures 5 and 6). The overall largest reduction is observed in the Pacific Northwest (~24% (+/−32%)), while the lowest reduction is observed in SR (~16% (+/−105%)). The average reduction over the last 33 years in the NR is approximately 23% (+/−32%). When considering severity gradients, at high fire severities, a larger reduction is observed compared to unburned areas (~25–59%) in all three ecodomains. The lowest reduction is observed with low-severity fires (~−7.4–10%). In the Southern Rockies, the burned areas associated with low-severity fires gained more biomass than the prefire level; however, they showed the largest variability.

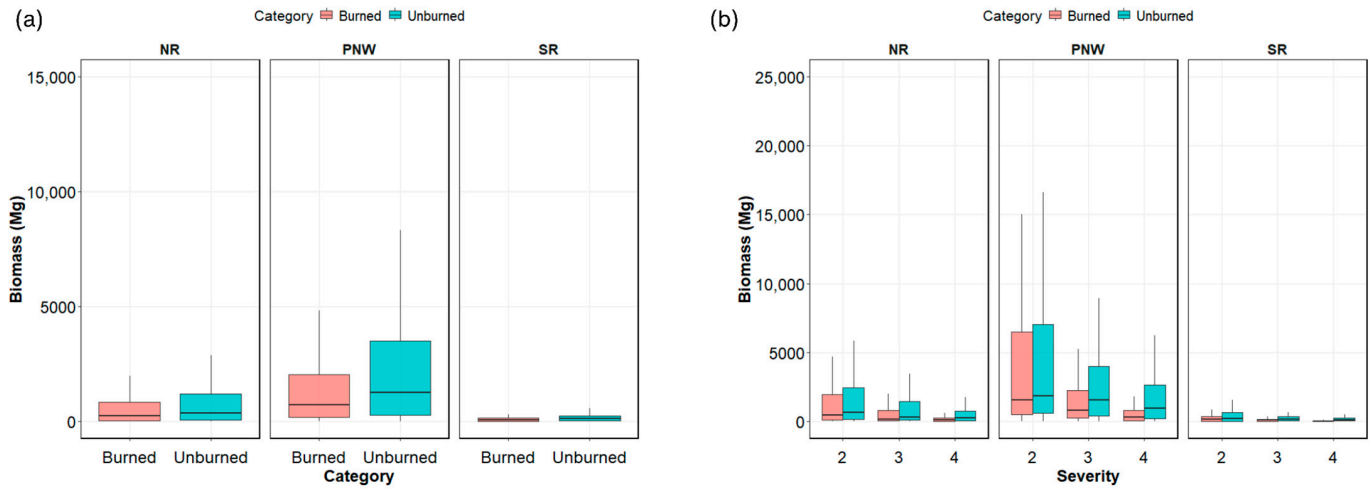

Figure 5. Total biomass at present time using cumulative biomass from all the fires studied, as well as all severity gradients compared to the estimate if they were not burned. (**a**) Total biomass comparison atecodomain scale; (**b**) biomass loss comparison at each severity gradient across three ecodomains.

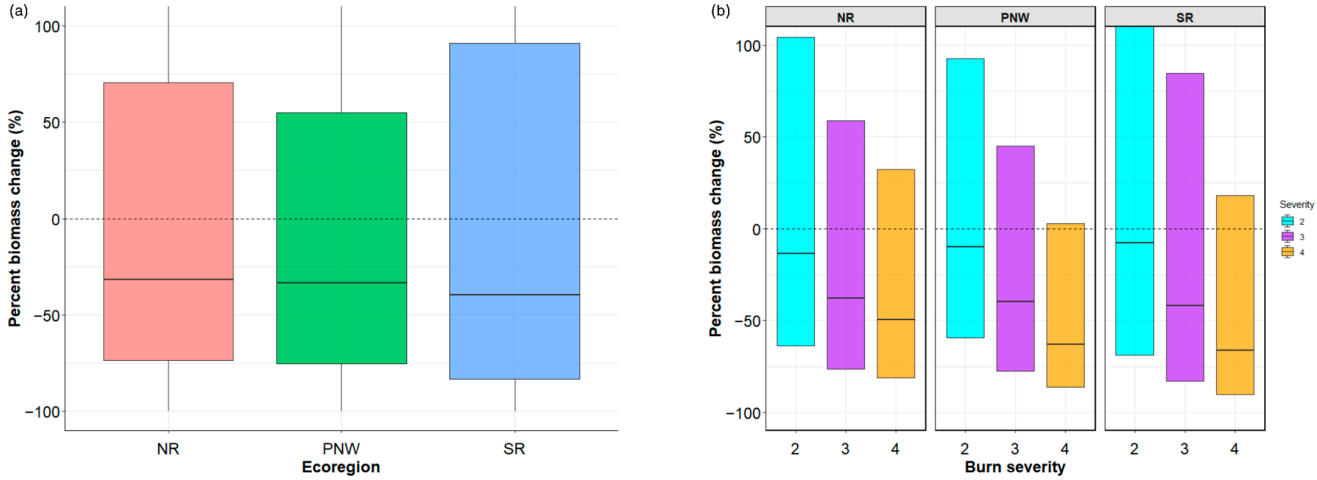

Figure 6. Percentage of biomass gain/loss due to wildfires in the studied ecodomains. The reduction is shown here as a negative value, and the positive value represents biomass gain compared to background state. (**a**) Percentage reduction in biomass compared to if the areas were not burned. (**b**) Percentage gain/loss at each severity level across each ecodomain.

4. Discussion

Tree burning and fire-driven mortality, followed by vegetation regeneration and succession, contribute to the future carbon potential of an ecosystem. Therefore, quantification of vegetation regeneration, succession timing, and trajectory after a fire is critical to estimate the ecosystem carbon stock and the global carbon balance, especially under changing climates. Postfire vegetation recovery trajectories were generated within three major western ecodomains for fires that occurred in the historically low- to moderate-severity fire regimes. The newest spaceborne lidar (i.e., GEDI)-based biomass density metrics over 390 fires across the western US between 1984 and 2017 were used in this study. This study evaluates biomass density and overall biomass changes within the first three decades of the postfire period as an estimate of carbon stocks and vegetation regrowth in the three main western US ecodomains. Further, this study evaluates the key drivers of the biomass recovery trajectory and the carbon potential of western US ecodomains after a fire.

This study used biomass density as the primary indicator of forest carbon stock recovery, as it directly relates to the balance between tree mortality and vegetation regrowth post-disturbance [51]. According to our results, the near-term (three decades postfire) biomass recovery is represented by a "U" shape curve, likely representing the initial and delayed tree mortality followed by vegetation regeneration and succession [52,53] unique to the low–moderate fire regimes in the western US. While some postfire regeneration studies use vegetation density as a regeneration metric [54–56], biomass density was used as a proxy for carbon gain postfire, as our main focus was to assess carbon recovery potential in these three ecodomains. The initial drop in biomass for all severity classes represents the biomass loss due to initial burning and near-snag falls.

Though this study selected burned areas within evergreen forests as the prefire dominant vegetation community, each burned area may contain other vegetation, including deciduous trees (e.g., aspen), as well as a range of combinations of coniferous vegetation communities with different growth rates. The shape of the postfire recovery trajectory largely depends on what species survived and regenerated under the disturbance. The slow decline in biomass in all severity classes in the PNW postfire may be due to other compounding disturbances, such as drought and beetle invasion, which can cause tree mortality for remaining unburned vegetation. In the PNW, ref. [57] showed that the rate of forest regeneration can follow multiple pathways for initial cohort development, and all these

pathways reach canopy closure in about four decades. The extrapolation of the recovery trajectory in our study, however, does not show full biomass recovery to pre-disturbance levels in the PNW even within the first five decades. Our results further support the previous findings where the postfire recovery of conifer forests in the Pacific Northwest (PNW) is increasingly hindered by changes in fire regimes, climate conditions, and forest composition. PNW forests dominated by Douglas fir (*Pseudotsuga menziesii*) and western hemlock (*Tsuga heterophylla*) have evolved under infrequent, high-severity fires [58]. These forests showed resilience due to long fire-free intervals that enabled recovery; however, recent contemporary fires, coupled with climate change and other anthropogenic influences, may have created conditions that impede the regeneration and recovery of this system.

In the NR ecodomain, our results are consistent with those of [56], as they show a larger reduction in standing trees from both stand-replacing (high severity) and non-replacing fires (low to moderate severity). The greater distance to seed sources can further reduce the postfire vegetation establishment [59]. The higher recovery rates associated with larger fire sizes may represent faster vegetation regeneration due to increased light and nutrient availability, especially aspen encroachment to postfire regions [60]. However, fire refugia size and spatial distribution, which may have an influence on promoting faster vegetation growth regardless of the fire size, were not considered in this study. Consistent with our findings, previous studies show that the fire severity within each stand can drive postfire vegetation recovery patterns in evergreen forests, with low-burn-severity regions showing a faster recovery, while the high-burn-severity regions show the slowest recovery [56]. In addition, stand-specific research in conifer forests yielded similar results [52], confirming the influence of site characteristics such as topography (elevation) on postfire recovery. The NR region is mainly dominated by fire-resistant Ponderosa pine (*Pinus ponderosa*) [32]. In addition, Quaking aspen (*Populus tremuloides*), a fire-tolerant deciduous species, can dominate burn scars [56] and replace conifer trees that were killed by beetle invasion. However, in high-severity fires, there will be limited seed availability for tree regeneration, leading to an open ecosystem with altered vegetation abundance and spatial structure. Research further shows that fire suppression during the past century in the NR has increased the fuel load in low elevations, while in high elevations, reduced snow packs have increased fire vulnerability [61]. This, coupled with the large influence of topography in postfire recovery, emphasizes the importance of future studies that evaluate how topography-related features such as slope, aspect, and elevation shape postfire vegetation recovery in the NR region.

The SR ecodomain comprises ponderosa pine, piñon–juniper woodland, high-elevation subalpine forests, as well as aspen, hence creating a variable fuel complex. The fast rate of regrowth in the low- and moderate-burn-severity regions in the SR could be due to an accelerated growth of existing vegetation due to the clearing (reduced competition for light). Our results show that in this ecodomain, fire severity, fire size, and the distance to unburned areas have a larger contribution to the biomass recovery trajectory shape than in the other two ecodomains. In agreement with our results, the authors of [54,62] also showed that postfire regeneration can fail with larger fires, especially in ponderosa pine-dominated regions.

This study considered areas that burned once, and did not consider compound disturbances, both at pre- and postfire stages, other than drought occurrences, following the evidence that the probability of invasion, such as beetle invasion, is minimal in postfire areas [63]. However, the frequency and magnitude of fire disturbance, together with other disturbances, define the distribution of vegetation composition in these ecodomains [27]. Evidence shows that tree mortality from increased mountain pine beetle invasion further reduces carbon stocks in the PNW region. Increased fire frequency, larger fires, and prefire

pine beetle invasion together can induce ecosystem state changes, converting forests into open vegetation and thus increasing carbon vulnerability in the western US. Hence, future studies that consider the impact of compound disturbance on vegetation recovery across ecodomains are essential to estimate the true carbon potential of these ecodomains.

5. Conclusions

Fire is a key regulator of forest carbon dynamics, and our results demonstrate that postfire biomass recovery across western U.S. conifer forests is increasingly delayed under contemporary fire regimes. Using GEDI-derived biomass estimates, this study shows that none of the studied ecodomains recover their prefire biomass within five decades, indicating persistent carbon deficits following fire. Recovery comparable to unburned conditions occurred only under low-severity fire consistent with historical regimes, whereas higher-severity fires affected 24–34% of burned areas and produced prolonged and divergent recovery trajectories. Biomass recovery was strongly ecodomain-specific, with faster recovery in the Southern Rockies and the slowest recovery in Pacific Northwest forests, and was primarily controlled by time since fire and fire severity, with additional influences from drought, elevation, fire size, and proximity to unburned refugia. These findings indicate that increasing fire severity in historically low-severity, high-frequency fire systems potentially represents a shift toward a novel fire regime. This will likely drive long-term reductions in forest carbon storage, underscoring the importance of management strategies that limit high-severity fires to sustain ecosystem resilience.

Supplementary Materials: The following supporting information can be downloaded at: https://www.mdpi.com/article/10.3390/fire9030096/s1, Figure S1: dNBR values of each ecoregion among MTBS burn severity groups after offset correction; Figure S2: Correlation between airborne lidar and GEDI lidar derived canopy heights in the western US evergreen forests; Figure S3: Spatiotemporal variability in drought conditions (mean SPEI) across ecoregions in each year; Figure S4: Standard deviation in drought conditions (mean SPEI) across fires in each year in each ecoregion.

Author Contributions: N.I. and J.K.B. conceptualized the study. N.I., J.K.B. and V.I. processed and analyzed data. N.I., J.K.B., R.C.N. and V.I. wrote the paper. All authors have read and agreed to the published version of the manuscript.

Funding: This study was supported by Earth Lab, Grand Challenge, and CIRES at the University of Colorado Boulder. Funding for this work was provided by the National Science Foundation CAREER Program grant 1846384 and the Environmental Data Science Innovation & Impact Lab (ESIIL) grant DBI-2153040.

Data Availability Statement: The data, models, and codes that support the findings of this study will be available with the publication of the manuscript. Please contact the corresponding author, Nayani Ilangakoon, via ginikanda.ilangakoon@colorado.edu. In addition, the GEDI footprint-based biomass density data are available at https://developers.google.com/earth-engine/datasets/catalog/LARSE_GEDI_GEDI04_A_002 (accessed on 19 January 2025). The fire occurrence, perimeter, and fire severity data are available at https://www.mtbs.gov/direct-download (accessed on 19 January 2025). The annual landcover data are available at https://www.mrlc.gov/data/project/annual-nlcd (accessed on 19 January 2025). The six-month means of standard precipitation evapotranspiration index (SPEI) data are available at https://spei.csic.es/database.html (accessed on 19 January 2025). The LANDFIRE fire regime groups data are available at https://www.landfire.gov/fire-regime/frg (accessed on 19 January 2025).

Conflicts of Interest: The authors declare that there were no conflicts of interest.

References

1. Pellegrini, A.F.A.; Ahlström, A.; Hobbie, S.E.; Reich, P.B.; Nieradzik, L.P.; Staver, A.C.; Scharenbroch, B.C.; Jumpponen, A.; Anderegg, W.R.L.; Randerson, J.T.; et al. Fire Frequency Drives Decadal Changes in Soil Carbon and Nitrogen and Ecosystem Productivity. *Nature* **2018**, *553*, 194–198. [CrossRef] [PubMed]
2. Walker, X.J.; Baltzer, J.L.; Bourgeau-Chavez, L.; Day, N.J.; Dieleman, C.M.; Johnstone, J.F.; Kane, E.S.; Rogers, B.M.; Turetsky, M.R.; Veraverbeke, S.; et al. Patterns of Ecosystem Structure and Wildfire Carbon Combustion Across Six Ecoregions of the North American Boreal Forest. *Front. For. Glob. Change* **2020**, *3*, 87. [CrossRef]
3. Birdsey, R.A. *Carbon Storage and Accumulation in United States Forest Ecosystems*; Department of Agriculture, Forest Service: Washington, DC, USA, 1992; Volume 59.
4. Buma, B. Disturbance Interactions: Characterization, Prediction, and the Potential for Cascading Effects. *Ecosphere* **2015**, *6*, 1–15. [CrossRef]
5. Stephens, S.L.; Agee, J.K.; Fulé, P.Z.; North, M.P.; Romme, W.H.; Swetnam, T.W.; Turner, M.G. Managing Forests and Fire in Changing Climates. *Science* **2013**, *342*, 41–42. [CrossRef]
6. Balch, J.K.; Bradley, B.A.; Abatzoglou, J.T.; Nagy, R.C.; Fusco, E.J.; Mahood, A.L. Human-Started Wildfires Expand the Fire Niche across the United States. *Proc. Natl. Acad. Sci. USA* **2017**, *114*, 2946–2951. [CrossRef]
7. Cattau, M.E.; Wessman, C.; Mahood, A.; Balch, J.K. Anthropogenic and Lightning-Started Fires Are Becoming Larger and More Frequent over a Longer Season Length in the USA. *Glob. Ecol. Biogeogr.* **2020**, *29*, 668–681. [CrossRef]
8. Abatzoglou, J.T.; Williams, A.P. Impact of Anthropogenic Climate Change on Wildfire across Western US Forests. *Proc. Natl. Acad. Sci. USA* **2016**, *113*, 11770–11775. [CrossRef]
9. Westerling, A.L. Increasing Western US Forest Wildfire Activity: Sensitivity to Changes in the Timing of Spring. *Philos. Trans. R. Soc. B Biol. Sci.* **2016**, *371*, 20150178. [CrossRef]
10. Iglesias, V.; Balch, J.K.; Travis, W.R. U.S. Fires Became Larger, More Frequent, and More Widespread in the 2000s. *Sci. Adv.* **2022**, *8*, eabc0020. [CrossRef]
11. Higuera, P.E.; Cook, M.C.; Balch, J.K.; Stavros, E.N.; Mahood, A.L.; St. Denis, L.A. Shifting Social-Ecological Fire Regimes Explain Increasing Structure Loss from Western Wildfires. *Proc. Natl. Acad. Sci. USA Nexus* **2023**, *2*, pgad005. [CrossRef]
12. Keeley, J.E. Fire Intensity, Fire Severity and Burn Severity: A Brief Review and Suggested Usage. *Int. J. Wildland Fire* **2009**, *18*, 116–126. [CrossRef]
13. Parks, S.A.; Miller, C.; Parisien, M.-A.; Holsinger, L.M.; Dobrowski, S.Z.; Abatzoglou, J. Wildland Fire Deficit and Surplus in the Western United States, 1984–2012. *Ecosphere* **2015**, *6*, 1–13. [CrossRef]
14. Davis, K.T.; Robles, M.D.; Kemp, K.B.; Higuera, P.E.; Chapman, T.; Metlen, K.L.; Peeler, J.L.; Rodman, K.C.; Woolley, T.; Addington, R.N.; et al. Reduced Fire Severity Offers Near-Term Buffer to Climate-Driven Declines in Conifer Resilience across the Western United States. *Proc. Natl. Acad. Sci. USA* **2023**, *120*, e2208120120. [CrossRef] [PubMed]
15. Coop, J.D.; Parks, S.A.; Stevens-Rumann, C.S.; Crausbay, S.D.; Higuera, P.E.; Hurteau, M.D.; Tepley, A.; Whitman, E.; Assal, T.; Collins, B.M.; et al. Wildfire-Driven Forest Conversion in Western North American Landscapes. *Bioscience* **2020**, *70*, 659–673. [CrossRef]
16. Johnstone, J.F.; Allen, C.D.; Franklin, J.F.; Frelich, L.E.; Harvey, B.J.; Higuera, P.E.; Mack, M.C.; Meentemeyer, R.K.; Metz, M.R.; Perry, G.L.; et al. Changing Disturbance Regimes, Ecological Memory, and Forest Resilience. *Front. Ecol. Environ.* **2016**, *14*, 369–378. [CrossRef]
17. Bartowitz, K.J.; Higuera, P.E.; Shuman, B.N.; McLauchlan, K.K.; Hudiburg, T.W. Post-Fire Carbon Dynamics in Subalpine Forests of the Rocky Mountains. *Fire* **2019**, *2*, 58. [CrossRef]
18. Turner, M.G.; Braziunas, K.H.; Hansen, W.D.; Hoecker, T.J.; Rammer, W.; Ratajczak, Z.; Westerling, A.L.; Seidl, R. The Magnitude, Direction, and Tempo of Forest Change in Greater Yellowstone in a Warmer World with More Fire. *Ecol. Monogr.* **2022**, *92*, e1485. [CrossRef]
19. Walker, X.J.; Rogers, B.M.; Veraverbeke, S.; Johnstone, J.F.; Baltzer, J.L.; Barrett, K.; Bourgeau-Chavez, L.; Day, N.J.; de Groot, W.J.; Dieleman, C.M.; et al. Fuel Availability Not Fire Weather Controls Boreal Wildfire Severity and Carbon Emissions. *Nat. Clim. Chang.* **2020**, *10*, 1130–1136. [CrossRef]
20. Finco, M.; Brad, Q.; Zhang, Y.; Lecker, J.; Megown, K.; Brewer, K.C. Monitoring Trends and Burn Severity (MTBS): Monitoring Wildfire Activity for the Past Quarter Century Using Landsat Data. In *Moving from Status to Trends: Forest Inventory and Analysis (FIA) Symposium 2012*; U.S. Department of Agriculture, Forest Service, Northern Research Station: Newtown Square, PA, USA, 2012; pp. 222–228.
21. Garcia, M.; Saatchi, S.; Casas, A.; Koltunov, A.; Ustin, S.; Ramirez, C.; Garcia-Gutierrez, J.; Balzter, H. Quantifying Biomass Consumption and Carbon Release from the California Rim Fire by Integrating Airborne LiDAR and Landsat OLI Data: C Released by the California Rim Fire. *J. Geophys. Res. Biogeosci.* **2017**, *122*, 340–353. [CrossRef]
22. Ilangakoon, N.T.; Glenn, N.F.; Dashti, H.; Painter, T.H.; Mikesell, T.D.; Spaete, L.P.; Mitchell, J.J.; Shannon, K. Constraining Plant Functional Types in a Semi-Arid Ecosystem with Waveform Lidar. *Remote. Sens. Environ.* **2018**, *209*, 497–509. [CrossRef]

23. Zhao, Y.; Zeng, Y.; Zheng, Z.; Dong, W.; Zhao, D.; Wu, B.; Zhao, Q. Forest Species Diversity Mapping Using Airborne LiDAR and Hyperspectral Data in a Subtropical Forest in China. *Remote. Sens. Environ.* **2018**, *213*, 104–114. [CrossRef]
24. Dubayah, R.; Blair, J.B.; Goetz, S.; Fatoyinbo, L.; Hansen, M.; Healey, S.; Hofton, M.; Hurtt, G.; Kellner, J.; Luthcke, S.; et al. The Global Ecosystem Dynamics Investigation: High-Resolution Laser Ranging of the Earth's Forests and Topography. *Sci. Remote Sens.* **2020**, *1*, 100002. [CrossRef]
25. Duncanson, L.; Armston, J.; Disney, M.; Avitabile, V.; Barbier, N.; Calders, K.; Carter, S.; Chave, J.; Herold, M.; Crowther, T.W.; et al. The Importance of Consistent Global Forest Aboveground Biomass Product Validation. *Surv. Geophys.* **2019**, *40*, 979–999. [CrossRef] [PubMed]
26. Ilangakoon, N.; Glenn, N.F.; Schneider, F.D.; Dashti, H.; Hancock, S.; Spaete, L.; Goulden, T. Airborne and Spaceborne Lidar Reveal Trends and Patterns of Functional Diversity in a Semi-Arid Ecosystem. *Front. Remote. Sens.* **2021**, *2*, 41. [CrossRef]
27. Hagmann, R.K.; Hessburg, P.F.; Prichard, S.J.; Povak, N.A.; Brown, P.M.; Fulé, P.Z.; Keane, R.E.; Knapp, E.E.; Lydersen, J.M.; Metlen, K.L.; et al. Evidence for Widespread Changes in the Structure, Composition, and Fire Regimes of Western North American Forests. *Ecol. Appl.* **2021**, *31*, e02431. [CrossRef]
28. Hann, W.; Shlisky, A.; Havlina, D.; Schon, K.; Barrett, S.; DeMeo, T.; Pohl, K.; Menakis, J.; Hamilton, D.; Jones, J.; et al. *Interagency Fire Regime Condition Class Guidebook*; Version 3.0; USDA Forest Service, US Department of the Interior: Washington, DC, USA; The Nature Conservancy: Arlington, VA, USA; Systems for Environmental Management: Missoula, MT, USA, 2010.
29. Kampe, T.U.; Johnson, B.R.; Kuester, M.A.; Keller, M. NEON: The First Continental-Scale Ecological Observatory with Airborne Remote Sensing of Vegetation Canopy Biochemistry and Structure. *J. Appl. Remote. Sens.* **2010**, *4*, 043510. [CrossRef]
30. Muthukrishnan, R.; Hayes, K.; Bartowitz, K.; Cattau, M.E.; Harvey, B.J.; Lin, Y.; Lunch, C. Harnessing NEON to Evaluate Ecological Tipping Points: Opportunities, Challenges, and Approaches. *Ecosphere* **2022**, *13*, e3989. [CrossRef]
31. Steel, Z.L.; Jones, G.M.; Collins, B.M.; Green, R.; Koltunov, A.; Purcell, K.L.; Sawyer, S.C.; Slaton, M.R.; Stephens, S.L.; Stine, P.; et al. Mega-Disturbances Cause Rapid Decline of Mature Conifer Forest Habitat in California. *Ecol. Appl.* **2022**, *33*, e2763. [CrossRef]
32. Keane, R.E.; Mahalovich, M.F.; Bollenbacher, B.L.; Manning, M.E.; Loehman, R.A.; Jain, T.B.; Holsinger, L.M.; Larson, A.J. Effects of Climate Change on Forest Vegetation in the Northern Rockies. In *Climate Change and Rocky Mountain Ecosystems*; Halofsky, J.E., Peterson, D.L., Eds.; Advances in Global Change Research; Springer International Publishing: Cham, Switzerland, 2018; Volume 63, pp. 59–95.
33. Eidenshink, J.; Schwind, B.; Brewer, K.; Zhu, Z.-L.; Quayle, B.; Howard, S. A Project for Monitoring Trends in Burn Severity. *Fire Ecol.* **2007**, *3*, 3–21. [CrossRef]
34. Fry, J.A.; Coan, M.J.; Homer, C.G.; Meyer, D.K.; Wickham, J.D. Completion of the National Land Cover Database (NLCD) 1992–2001 Land Cover Change Retrofit Product. *US Geol. Surv. Open-File Rep.* **2008**, *1379*, 18. [CrossRef]
35. Homer, C.; Dewitz, J.; Jin, S.; Xian, G.; Costello, C.; Danielson, P.; Gass, L.; Funk, M.; Wickham, J.; Stehman, S.; et al. Conterminous United States Land Cover Change Patterns 2001–2016 from the 2016 National Land Cover Database. *ISPRS J. Photogramm. Remote. Sens.* **2020**, *162*, 184–199. [CrossRef] [PubMed]
36. Sohl, T.; Dornbierer, J.; Wika, S.; Robison, C. Remote Sensing as the Foundation for High-Resolution United States Landscape Projections—The Land Change Monitoring, Assessment, and Projection (LCMAP) Initiative. *Environ. Model. Softw.* **2019**, *120*, 104495. [CrossRef]
37. Schlund, M.; Wenzel, A.; Camarretta, N.; Stiegler, C.; Erasmi, S. Vegetation Canopy Height Estimation in Dynamic Tropical Landscapes with TanDEM-X Supported by GEDI Data. *Methods Ecol. Evol.* **2022**, *14*, 1639–1656. [CrossRef]
38. Parks, S.A.; Holsinger, L.M.; Voss, M.A.; Loehman, R.A.; Robinson, N.P. Mean Composite Fire Severity Metrics Computed with Google Earth Engine Offer Improved Accuracy and Expanded Mapping Potential. *Remote. Sens.* **2018**, *10*, 879. Correction in *Remote Sens.* **2021**, *13*, 4580. https://doi.org/10.3390/rs13224580. [CrossRef]
39. Kolden, C.A.; Smith, A.M.S.; Abatzoglou, J.T. Limitations and Utilisation of Monitoring Trends in Burn Severity Products for Assessing Wildfire Severity in the USA. *Int. J. Wildland Fire* **2015**, *24*, 1023–1028. [CrossRef]
40. Duncanson, L.; Neuenschwander, A.; Hancock, S.; Thomas, N.; Fatoyinbo, T.; Simard, M.; Silva, C.A.; Armston, J.; Luthcke, S.B.; Hofton, M.; et al. Biomass Estimation from Simulated GEDI, ICESat-2 and NISAR across Environmental Gradients in Sonoma County, California. *Remote. Sens. Environ.* **2020**, *242*, 111779. [CrossRef]
41. Welty, J.; Jeffries, M. *Combined Wildland Fire Datasets for the United States and Certain Territories, 1800s-Present*; Forest and Rangeland Ecosystem Science Center (FRESC) Headquarters: Corvallis, OR, USA, 2021.
42. Beguería, S. *Sbegueria/SPEIbase*, Version 2.7; Consejo Superior de Investigaciones Científicas: Madrid, Spain, 2022. [CrossRef]
43. Hérault, B.; Piponiot, C. Key Drivers of Ecosystem Recovery after Disturbance in a Neotropical Forest: Long-Term Lessons from the Paracou Experiment, French Guiana. *For. Ecosyst.* **2018**, *5*, 2. [CrossRef]
44. Bright, B.C.; Hudak, A.T.; Kennedy, R.E.; Braaten, J.D.; Henareh Khalyani, A. Examining Post-Fire Vegetation Recovery with Landsat Time Series Analysis in Three Western North American Forest Types. *Fire Ecol.* **2019**, *15*, 8. [CrossRef]

45. Magnussen, S.; Wulder, M.A. Post-Fire Canopy Height Recovery in Canada's Boreal Forests Using Airborne Laser Scanner (ALS). *Remote. Sens.* **2012**, *4*, 1600–1616. [CrossRef]
46. Chambers, M.E.; Fornwalt, P.J.; Malone, S.L.; Battaglia, M.A. Patterns of Conifer Regeneration Following High Severity Wildfire in Ponderosa Pine—Dominated Forests of the Colorado Front Range. *For. Ecol. Manag.* **2016**, *378*, 57–67. [CrossRef]
47. Palviainen, M.; Laurén, A.; Pumpanen, J.; Bergeron, Y.; Bond-Lamberty, B.; Larjavaara, M.; Kashian, D.M.; Köster, K.; Prokushkin, A.; Chen, H.Y.H.; et al. Decadal-Scale Recovery of Carbon Stocks After Wildfires Throughout the Boreal Forests. *Glob. Biogeochem. Cycles* **2020**, *34*, e2020GB006612. [CrossRef]
48. Akaike, H. Information Theory and an Extension of the Maximum Likelihood Principle. In *Selected Papers of Hirotugu Akaike*; Parzen, E., Tanabe, K., Kitagawa, G., Eds.; Springer Series in Statistics; Springer: New York, NY, USA, 1998; pp. 199–213.
49. Wood, S.N. Stable and Efficient Multiple Smoothing Parameter Estimation for Generalized Additive Models. *J. Am. Stat. Assoc.* **2004**, *99*, 673–686. [CrossRef]
50. Nigro, K.M.; Rocca, M.E.; Battaglia, M.A.; Coop, J.D.; Redmond, M.D. Wildfire Catalyzes Upward Range Expansion of Trembling Aspen in Southern Rocky Mountain Beetle-Killed Forests. *J. Biogeogr.* **2022**, *49*, 201–214. [CrossRef]
51. Frolking, S.; Palace, M.W.; Clark, D.B.; Chambers, J.Q.; Shugart, H.H.; Hurtt, G.C. Forest Disturbance and Recovery: A General Review in the Context of Spaceborne Remote Sensing of Impacts on Aboveground Biomass and Canopy Structure. *J. Geophys. Res. Biogeosci.* **2009**, *114*, 2008JG000911. [CrossRef]
52. Tepley, A.J.; Thompson, J.R.; Epstein, H.E.; Anderson-Teixeira, K.J. Vulnerability to Forest Loss through Altered Postfire Recovery Dynamics in a Warming Climate in the Klamath Mountains. *Glob. Chang. Biol.* **2017**, *23*, 4117–4132. [CrossRef] [PubMed]
53. Tepley, A.J.; Veblen, T.T. Spatiotemporal Fire Dynamics in Mixed-Conifer and Aspen Forests in the San Juan Mountains of Southwestern Colorado, USA. *Ecol. Monogr.* **2015**, *85*, 583–603. [CrossRef]
54. Boucher, D.; Gauthier, S.; Thiffault, N.; Marchand, W.; Girardin, M.; Urli, M. How Climate Change Might Affect Tree Regeneration Following Fire at Northern Latitudes: A Review. *New For.* **2020**, *51*, 543–571. [CrossRef]
55. Stevens, J.T.; Kling, M.M.; Schwilk, D.W.; Varner, J.M.; Kane, J.M. Biogeography of Fire Regimes in Western U.S. Conifer Forests: A Trait-Based Approach. *Glob. Ecol. Biogeogr.* **2020**, *29*, 944–955. [CrossRef]
56. Stevens-Rumann, C.S.; Hudak, A.T.; Morgan, P.; Arnold, A.; Strand, E.K. Fuel Dynamics Following Wildfire in US Northern Rockies Forests. *Front. For. Glob. Chang.* **2020**, *3*, 51. [CrossRef]
57. Whitlock, C.; McWethy, D.B.; Tepley, A.J.; Veblen, T.T.; Holz, A.; McGlone, M.S.; Perry, G.L.W.; Wilmshurst, J.M.; Wood, S.W. Past and Present Vulnerability of Closed-Canopy Temperate Forests to Altered Fire Regimes: A Comparison of the Pacific Northwest, New Zealand, and Patagonia. *BioScience* **2015**, *65*, 151–163. [CrossRef]
58. Tepley, A.J.; Swanson, F.J.; Spies, T.A. Fire-Mediated Pathways of Stand Development in Douglas-Fir/Western Hemlock Forests of the Pacific Northwest, USA. *Ecology* **2013**, *94*, 1729–1743. [CrossRef]
59. Harvey, B.J.; Donato, D.C.; Turner, M.G. Recent Mountain Pine Beetle Outbreaks, Wildfire Severity, and Postfire Tree Regeneration in the US Northern Rockies. *Proc. Natl. Acad. Sci. USA* **2014**, *111*, 15120–15125. [CrossRef]
60. Romme, W.H.; Turner, M.G.; Tuskan, G.A.; Reed, R.A. ESTABLISHMENT, PERSISTENCE, AND GROWTH OF ASPEN (POPULUS TREMULOIDES) SEEDLINGS IN YELLOWSTONE NATIONAL PARK. *Ecology* **2005**, *86*, 404–418. [CrossRef]
61. Reis, W.; Turner, M.; Tuskan, G.; Reed, R. Quantifying Aspect-Dependent Snowpack Response to High-Elevation Wildfire in the Southern Rocky Mountains. Ph.D. Thesis, Colorado State University, Fort Collins, CO, USA, 2023; p. 30566329.
62. Hammond, D.H.; Strand, E.K.; Morgan, P.; Hudak, A.T.; Newingham, B.A. Environmental Influences on Density and Height Growth of Natural Ponderosa Pine Regeneration Following Wildfires. *Fire* **2021**, *4*, 80. [CrossRef]
63. Holliday, N. SPECIES RESPONSES OF CARABID BEETLES (COLEOPTERA: CARABIDAE) DURING POST-FIRE REGENERATION OF BOREAL FOREST. *Can. Èntomol.* **1991**, *123*, 1369–1389. [CrossRef]